Poloidal Field System Analysis
and Scenario Development
for the TIBER/ITER

Joel H. Schultz
M.I.T. Plasma Fusion Center

R. Bulmer, J. Miller, and J. Perkins
Lawrence Livermore National Laboratory

Poloidal Field System Analysis and Scenario Development for the TIBER/ITER

Joel H. Schultz

M.I.T. Plasma Fusion Center

R. Bulmer, J. Miller, and J. Perkins

Lawrence Livermore Laboratory

1.0 Introduction

TIBER is the United States' contribution to the design of an international thermonuclear experimental reactor (ITER). The poloidal field (PF) magnets are responsible for forming and shaping highly elongated, high-current plasmas, during a long-pulse burn. A variety of experiments must be supported by the PF system design, including steady-state burn with current drive, all inductive, high-performance, short-burn, long-burn discharges with partial current drive, and ohmic burn with transformer reset by rf current drive.

The PF coils are superconducting, using high field, Nb_3Sn superconductor with titanium additives. The conductor/winding pack topology is potted, internally-cooled cabled superconductor (ICCS), circulating supercritical helium. The field and pulsed-loss requirements are higher for the PF system than for the toroidal field (TF) system, although the steady-state heat removal requirement is not as high. The PF coils are designed up to maximum fields of 14 T and field-current density products of 500 MAT/m^2. These limits are reached at the beginning of initiation, the beginning of burn and the end of burn in a typical scenario. In a scenario with rf reset, limits are reached at the beginning and end of low-beta reset.

2.0 Pulsed Inductive Operation

2.1 PF Scenarios

Poloidal field scenarios have been developed for several options. This report concentrates on the ohmic start-up and burn scenario for an 8 MA plasma and a similar scenario with lower hybrid transformer reset. The 3.0 m TIBER plasma can be driven to 8 MA ohmically and the plasma can be sustained for an additional 10 V-s with no assistance from rf power sources. The scenario illustrated here assumes 10 V-s of rf assist, allowing a 20 V-s burn, which is the limit of the PF capability, independent of the rf assist during start-up.

The scenario satisfies the physics and engineering constraints described in Table I. The PF currents also provide high-beta MHD equilibria at the beginning and end of burn and a broad field null at the beginning of initiation. The PF coil set is described in Table II and illustrated in Fig. 1.

Table I
Poloidal Field System Constraints

I_p	8.0	(MA)
$V\text{-}S_{su,norf}$	48	(Wb)
V_{init}	21	(V)
B_{max}	14	(T)
JB_{max}	500	MA-T/m^2
$\sigma_{Trescamembrane}$	800	(MPa)
$V_{terminal}$	20	(kV)
I_{cond}	25	(kA)

Table II
TIBER PF System Winding Pack Dimension

Coil	R (m)	Z (m)	R_1 (m)	R_2 (m)	Z_1 (m)	Z_2 (m)	n_{turns}
PF1,U,L	6.2	± 1.5	6.0	6.4	± 1.3	± 1.7	300
PF2,U,L	6.2	± 3.2	6.0	6.4	± 3.0	± 3.4	150
PF3,U,L	4.1	± 4.25	3.9	4.3	± 4.05	± 4.45	120
PF4,U,L	1.8	± 4.25	1.6	2.0	± 4.05	± 4.45	300
PF5+6,U,L	0.8	± 2.8	0.6	1.0	± 2.412	± 3.188	600
PF7+8,U,L	0.8	± 2.0	0.6	1.0	± 1.613	± 2.388	600
PF9+10,U,L	0.8	± 1.2	0.6	1.0	± 0.813	± 1.588	600
PF11+12,U,L	0.8	± 0.4	0.6	1.0	± 0.013	± 0.788	600

OVERALL ASSEMBLY-62
TIBER2 7-21-87
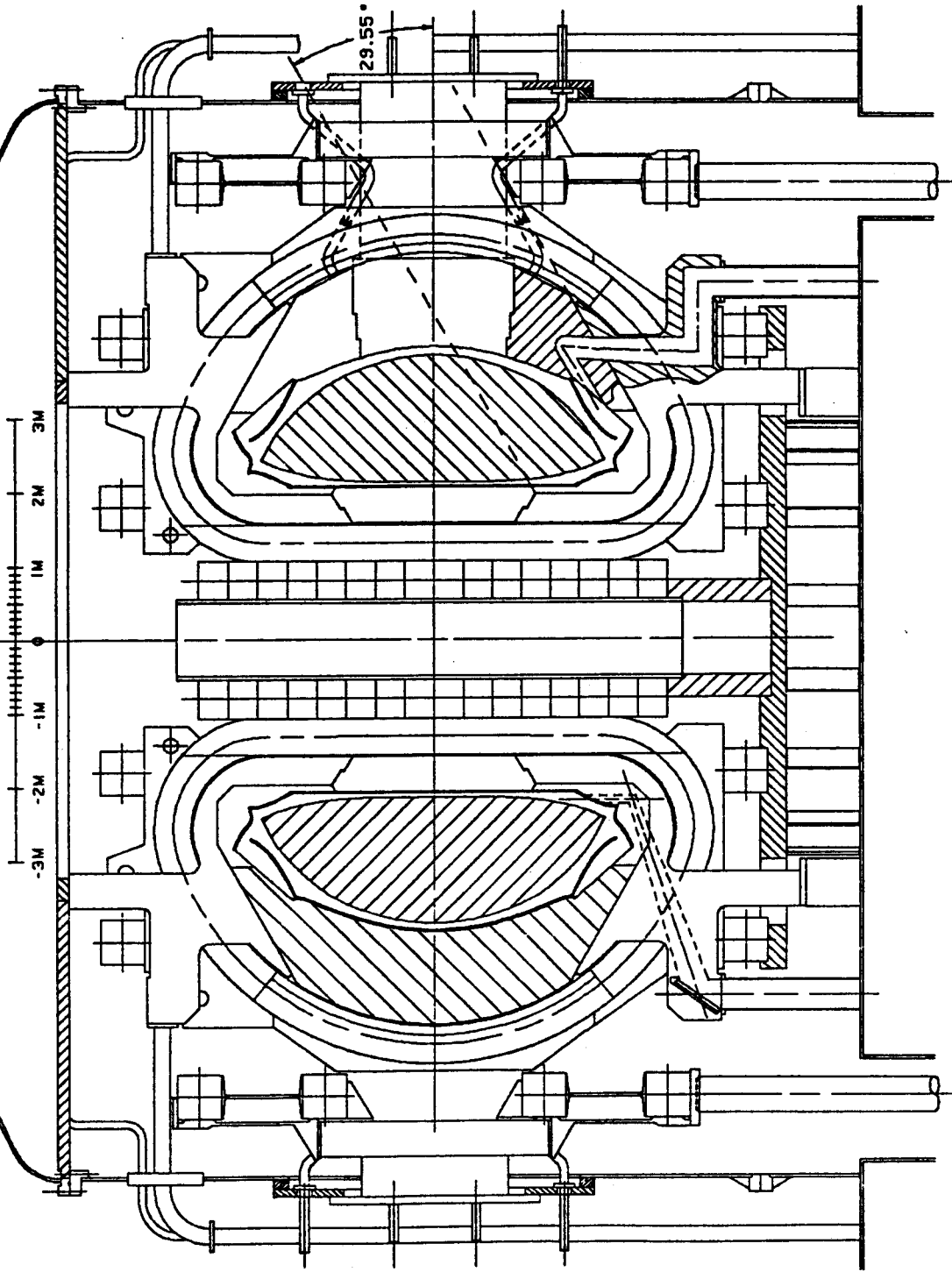
29.55°

3M
2M
1M
0
-1M
-2M
-3M

Fig. 1 – Elevation View of TIBER

The contributions of the various PF coils to the plasma volt-seconds are shown in Fig. 2. The largest individual contribution is from PF1, the outside vertical field coil. The loop voltage provided to the plasma for initiation is 21 V for 50 ms, which is aggressive in comparison with the designs of tokamaks not using any rf assist. However, there are large amounts of rf power available for initiation assistance, if needed.

The twenty-four poloidal field coils are driven by eight symmetric power supplies. Peak currents and voltages in the PF coils have been held below 25 kA and 20 kV, respectively. The peak current and voltage are both on PF1, the outside vertical field coil. The PF1 negative current supply requires 2494 V, which requires seriesing of the rectifiers. The other power supplies have the option of paralleling for greater passive vertical stability or seriesing, without exceeding the capabilities of the rectifiers.

2.2 Constraints

A survey of the performance of high-performance solenoids and selected toroidal magnets was made. The survey suggests the use of a minimum of three performance limits at the conceptual design level: B_{max}, JB_{max}, and $JB_{max}R$. These are dimensionally similar to the limits agreed upon in a community review in 1984 for the TFCX project [PP84], but what was considered aggressive then is conservative now. A comparison of the previous recommendations with those used in the TIBER design is shown in Table III. The sizing of the TIBER PF system is based on the right-hand column, which corresponds to the goals of the U.S.-Japan Multipurpose Coil Task.

Table III
Comparison of TIBER with TFCX Allowables

Allowable	Units	1984 Conservative	1984 Aggressive	Benchmarked	1987 Planned	1987
B_{max}	(T)	8	12	12	14	
JB_{max} (MA-T/m^2		160	260	450	550	
JBR	(MA-T/m)	420	462	290	380	

2.3 Method

A new PF trades code was developed to explore the limitations of a superconducting coil system with no constraints on plasma volt-second requirements. This permits the sizing of a broad range of experiments from full ohmic to full steady-state current drive.

VS,max (Wb) = 22.841
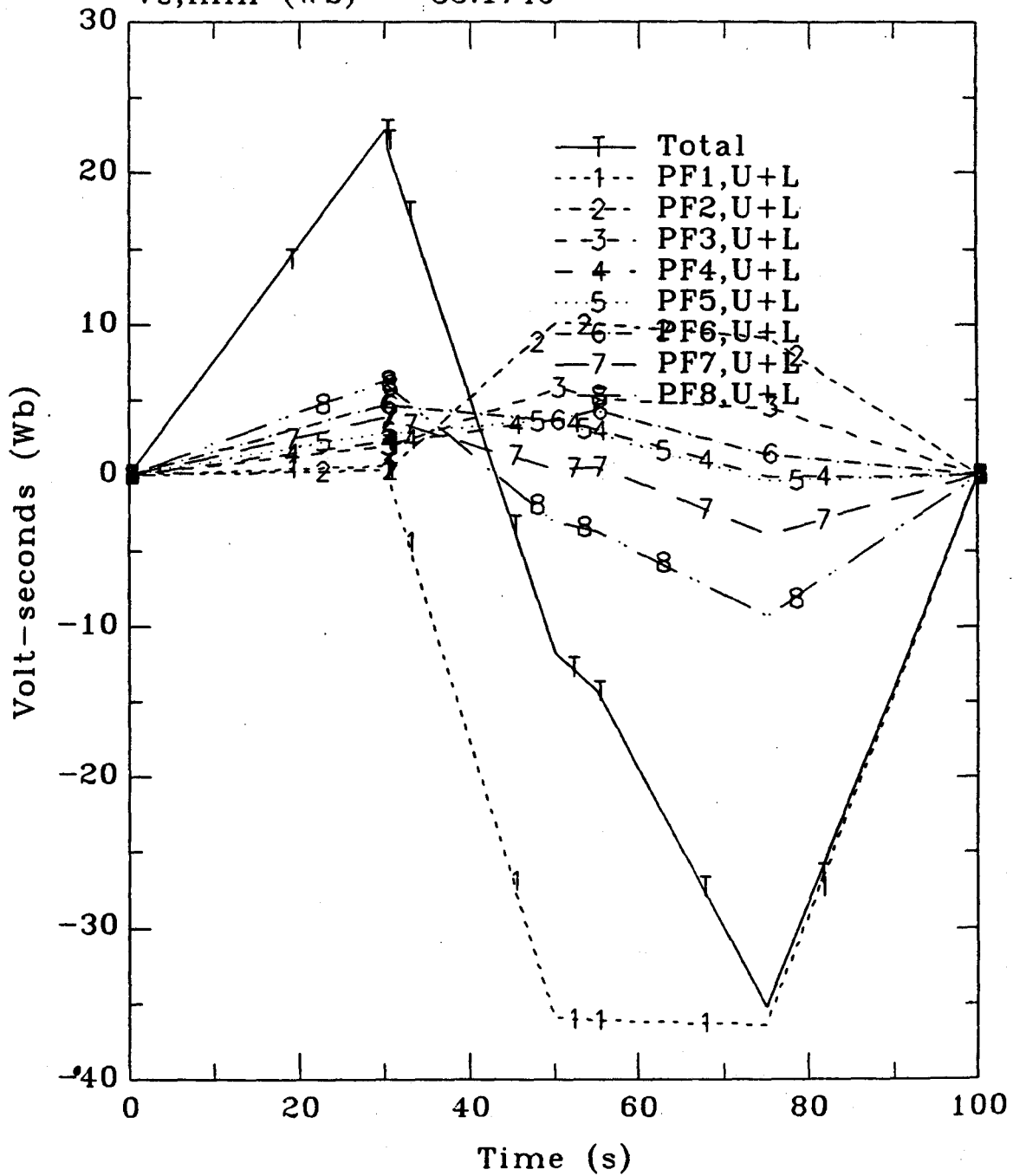Vs,min (Wb) = −35.1749

Fig. 2 − PF Coil Contributions to Plasma Volt-Seconds

5

After the survey established a set of design allowables, the flux bias and volt-second swing were varied and compared with the abovementioned allowables. This analysis showed limits not only on poloidal field flux at the beginning of initiation and at the end of burn, but also at the beginning of burn. This limit was not located at the equator of the central solenoid, but at its tips in the divertor region.

3.0 Time History

A time scenario of the coil currents was developed that satisfied the magnet and physics constraints for the ohmic start-up and burn of an 8 MA plasma. The currents selected produce a scenario that reaches allowable limits at three points in time: preinitiation, beginning of burn, and end of burn. The characteristic triple peak in B_{max} is seen in Fig. 3. The peak field, while generally in the ohmic solenoid stack is not necessarily at the equator, but moves up and down the stack during a discharge. At the beginning of burn, when the divertor coil currents are highest, the peak field limitation is at the top of the solenoid stack. The same pattern is shown in the constraint on JB_{max}. Stress limits are much more complex, because of the constraints on fatigue life, the complex load path in the TIBER central solenoid stack, and local bending in the ICCS conduit walls.

The minimum fraction of critical current within each coil was also calculated as a function of time. The equations for critical current and temperature were derived from the Tiber Final Design Report [HE85], being Miller's interpretation of Suenaga's data on MF-Nb_3Sn conductor with titanium additions [SU85]. The highest fraction of conductor critical current in the 8 MA scenario is 0.45 in PF5, the top of the central solenoid, at the beginning of burn.

3.1 <u>Power and Energy Requirements</u>

The power and energy required from external power supplies are shown in Fig. 4. The energy requirements are modest, compared with CIT, because of the absence of resistive losses in the superconductors and are small compared with other proposed superconducting tokamaks, such as NET or FER, because of the smaller size. The peak energy requirement is 1680 MJ at the beginning of burn. The dominant coil is PF1, the outside ring coil which provides most of the vertical field. The maximum positive power of 123 MW must be provided by a utility or local generator. The peak negative power of -604 MW during initiation can be dumped in external resistors. As with the energy, line power is dominated by PF1, the outside ring coil, while the negative power at initiation is dominated by the central solenoid stack (PF5-12).
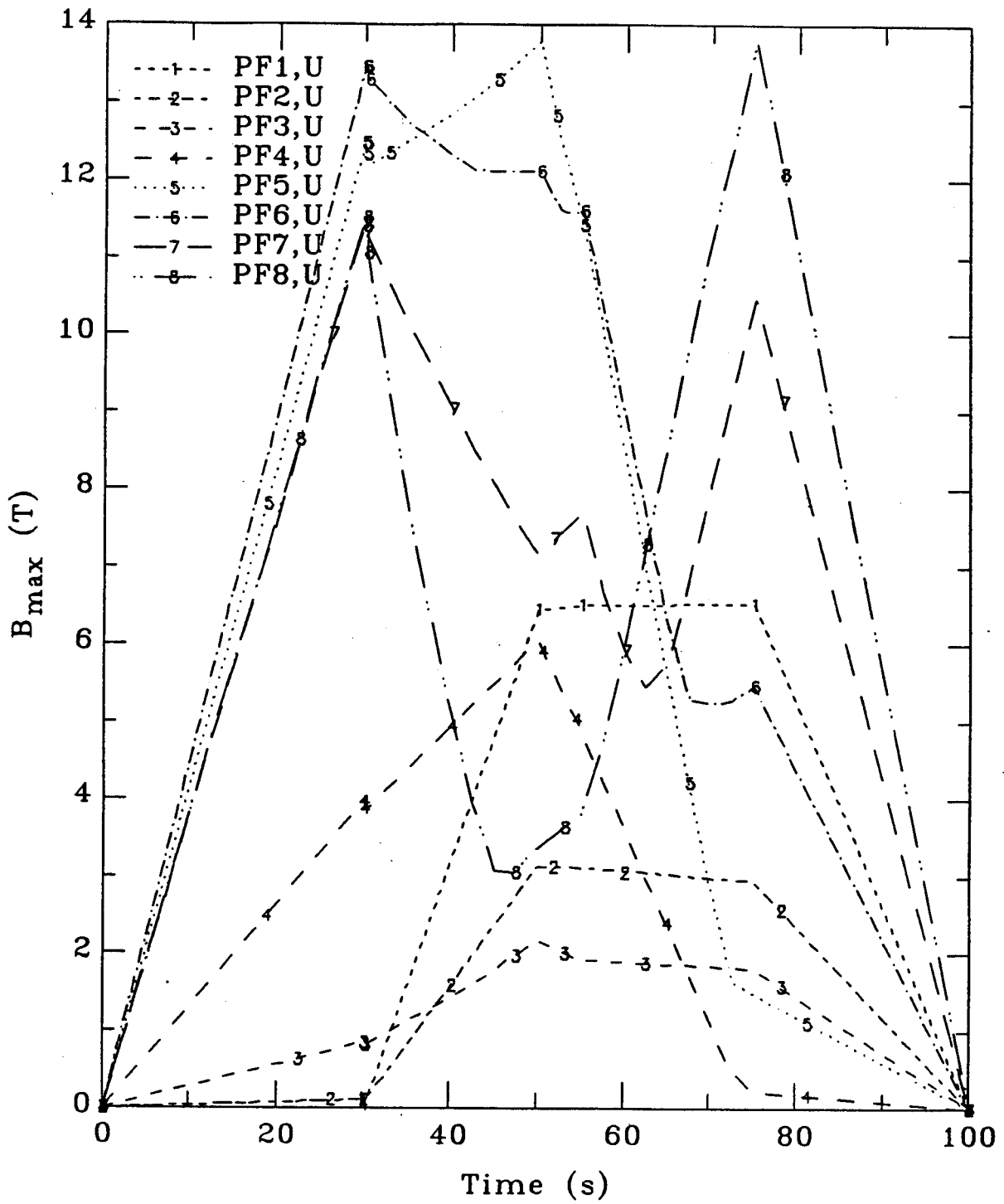
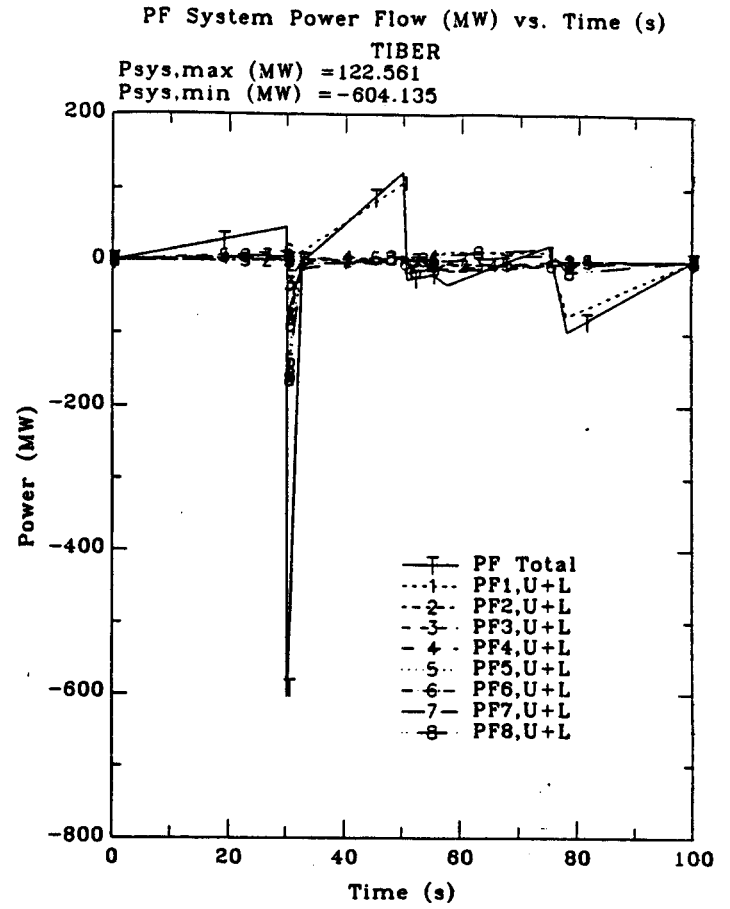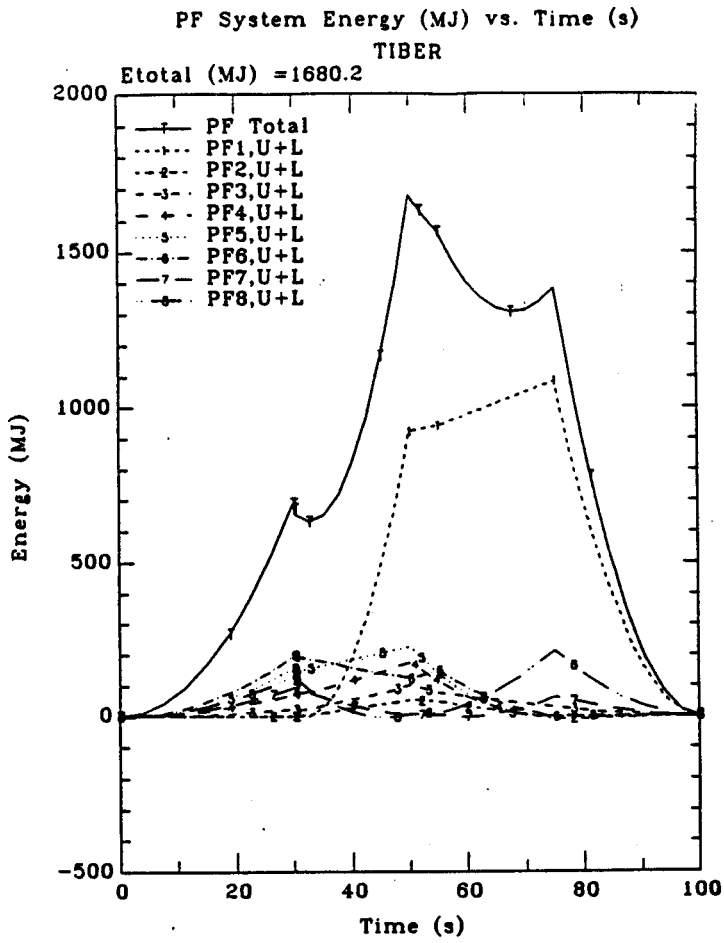Fig. 3 – Maximum Field in PF Coils (T) vs Time (s)

PF System Energy (MJ) vs. Time (s)
TIBER
Etotal (MJ) = 1680.2

Legend:
- ⊥ PF Total
- ···1··· PF1,U+L
- ·–2–· PF2,U+L
- – –3– – PF3,U+L
- – ← – PF4,U+L
- ······5······ PF5,U+L
- –·4·– PF6,U+L
- —7— PF7,U+L
- ···8··· PF8,U+L

Energy (MJ)

Time (s)

PF System Power Flow (MW) vs. Time (s)
TIBER
Psys,max (MW) = 122.561
Psys,min (MW) = -604.135

Legend:
- ⊥ PF Total
- ···1··· PF1,U+L
- ··2·· PF2,U+L
- – –3– – PF3,U+L
- – 4 – PF4,U+L
- ·····5····· PF5,U+L
- –·6·– PF6,U+L
- —7— PF7,U+L
- ··8·· PF8,U+L

Power (MW)

Time (s)

Figure 4
TIBER Power and Energy Requirements

8

3.2 Load History

The hoop and vertical loads on each coil were calculated at each point in time. The average Tresca membrane stress in the conductor conduit was calculated at each point in time. The total load on each coil following either a disruption or a coil fault has been calculated for faults at the beginning of initiation and the end of burn for current-conserving and flux-conserving faults. Even if all coils were entirely self-supporting, all coils would be within the static membrane allowable (2/3 yield stress of JBK-75 in the conduit), before and after disruption. The highest Tresca membrane stress in a self-supporting conduit would be 730 MPa in PF1, which is close to the static allowable of 800 MPa. PF1 is on the outside of the machine and could be enlarged, if desired. In the central solenoid, where space is more constrained, the self-supporting Tresca membrane stress is 700 MPa, at the beginning of initiation, but the hoop tension stress of 530 MPa would be largely canceled by compression from the TF coils, greatly improving the fatigue life of the central solenoid with some degradation in critical properties.

3.3 Pulsed Losses

Pulsed losses in the PF system have several large components, none of which are clearly dominant. Losses in the PF windings are caused by superconducting hysteresis and transverse coupling. Pulsed losses in the cases are considered for transverse field pulses and induced electric fields. If there are no insulating breaks in the cases, the losses under a normal scenario due to parallel electric fields will be about five times higher than those due to pulsed magnetic fields.

The pulsed losses in the PF winding packs and cases during a normal scenario have been calculated. Losses in the winding packs and cases are shown in Fig. 5. The total system loss is 9 MJ. Losses in the central solenoid, PF5-8, are dominant, with each of the four central- solenoid modules making a significant contribution. Over one-third of the losses are deposited during initiation. For a reference burn time of 200 s, the TF neutron and gamma losses are 14.4 MJ, comparable to the PF pulsed-field losses. The total loss in the cases is 11 MJ, with losses in the central solenoid dominant. Over half of the losses are deposited during initiation. For a 300 second overall cycle time, which would give a 2/3 local duty factor, the cryogenic refrigeration plant for the poloidal-field system would be rated at 67 kW, which is comparable to the requirement for the TF system.

The losses in a disruption have been calculated by two methods, assuming that each PF coil conserves either current or flux. The accumulated losses before and after disruption for either assumption are calculated at every point in time for the PF winding packs, as
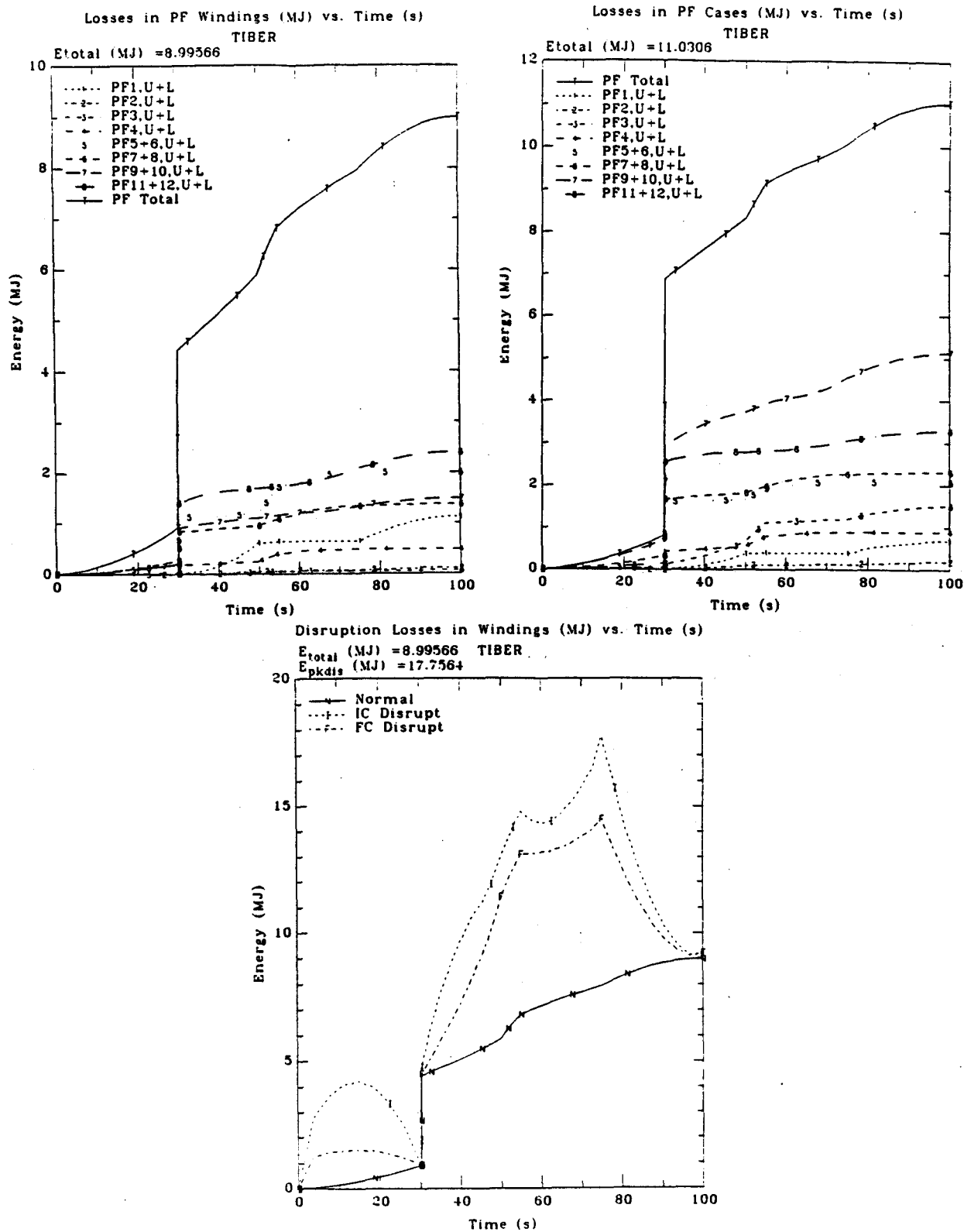
9

Losses in PF Windings (MJ) vs. Time (s)
TIBER
Etotal (MJ) =8.99566

Legend:
- ······· PF1,U+L
- -·2·- PF2,U+L
- -·3·- PF3,U+L
- -·4·- PF4,U+L
- 5 PF5+6,U+L
- -·6·- PF7+8,U+L
- -·7·- PF9+10,U+L
- ·●· PF11+12,U+L
- ·+· PF Total

Losses in PF Cases (MJ) vs. Time (s)
TIBER
Etotal (MJ) =11.0306

Legend:
- ·+· PF Total
- ······· PF1,U+L
- -·2·- PF2,U+L
- -·3·- PF3,U+L
- -·4·- PF4,U+L
- 5 PF5+6,U+L
- -·6·- PF7+8,U+L
- -·7·- PF9+10,U+L
- ·●· PF11+12,U+L

Disruption Losses in Windings (MJ) vs. Time (s)
E_{total} (MJ) =8.99566   TIBER
E_{pkdis} (MJ) =17.7564

Legend:
- ·▲· Normal
- ···f··· IC Disrupt
- ·-f-· FC Disrupt

Fig. 5 – Pulsed Losses in PF Winding Packs and Cases

10

shown in Fig. 5. The worst time for a disruption for either the current-conserving or the flux-conserving model is at the end of burn. If a current-conserving disruption occurred at the end of burn, a total of 17.8 MJ would be deposited in the winding packs, nearly double the normal end of discharge total. If a flux-conserving disruption occurred at the end of burn, the peak dissipation would be 14.8 MJ.

4.0 Scenario with RF Reset

The intent of the TIBER design has been to reset the plasma flux linkage, using lower hybrid current drive at low density. The motivation for using rf reset, instead of the conventional full ohmic reset, is to minimize the stress cycles on the magnets and other structures, thus avoiding high-cycle structural fatigue limits. The scenario described below represents the first self-consistent rf reset scenario meeting physics and engineering constraints.

A set of PF coil currents was developed, interpolating from two pairs of full-current MHD equilibria at high and low beta. Poloidal field currents were then varied through ranges that preserved the two equilibria, while varying flux linkage, in order to find the limits of the PF system. For the equilibria studied, the magnets were constrained by the low beta equilibria at both the high and the low flux linkage limits. Thus, although the PF magnet set is capable of a flux swing of 20 V-s at high beta and 8 MA, it is only capable of a flux swing of 10 V-s at low beta and 8 MA. The transitions between high and low beta allocate 1 V-s apiece, leaving 8 V-s for the high-beta ignited burn. A scenario with one start-up, two flattops, one reset, and one shutdown is shown in Fig. 6. PF1, the main equilibrium field coil, provides most of the transition flux from high to low beta and back, while the central solenoid, PF5-12, is responsible for most of the flux reset. At the beginning of flux reset, the central solenoid reaches a current density-flux density product of 480 MAT-T/m^2 and a flux density of 13.8 T, while PF4, in the divertor region, reaches a current density-flux density product of 490 MAT-T/m^2 at the end of reset, as shown in Fig. 7. The limitation on PF4 could be relieved by making the coil taller, since its flux density is only 9 T at this point. This should extend the ignited burn period by another 6.5 V-s.

As shown in Fig. 8, the power requirements for the PF system are modest, as they were for full ohmic reset. However, with 10 s apiece allocated for the transitions between high and low beta, the power requirement for transition is as high as that required for start-up. For a given set of power supplies, this is another limitation on the duty factor achievable with rf reset. The power supply for the PF4 coil has to be increased substantially over that required for ohmic reset.
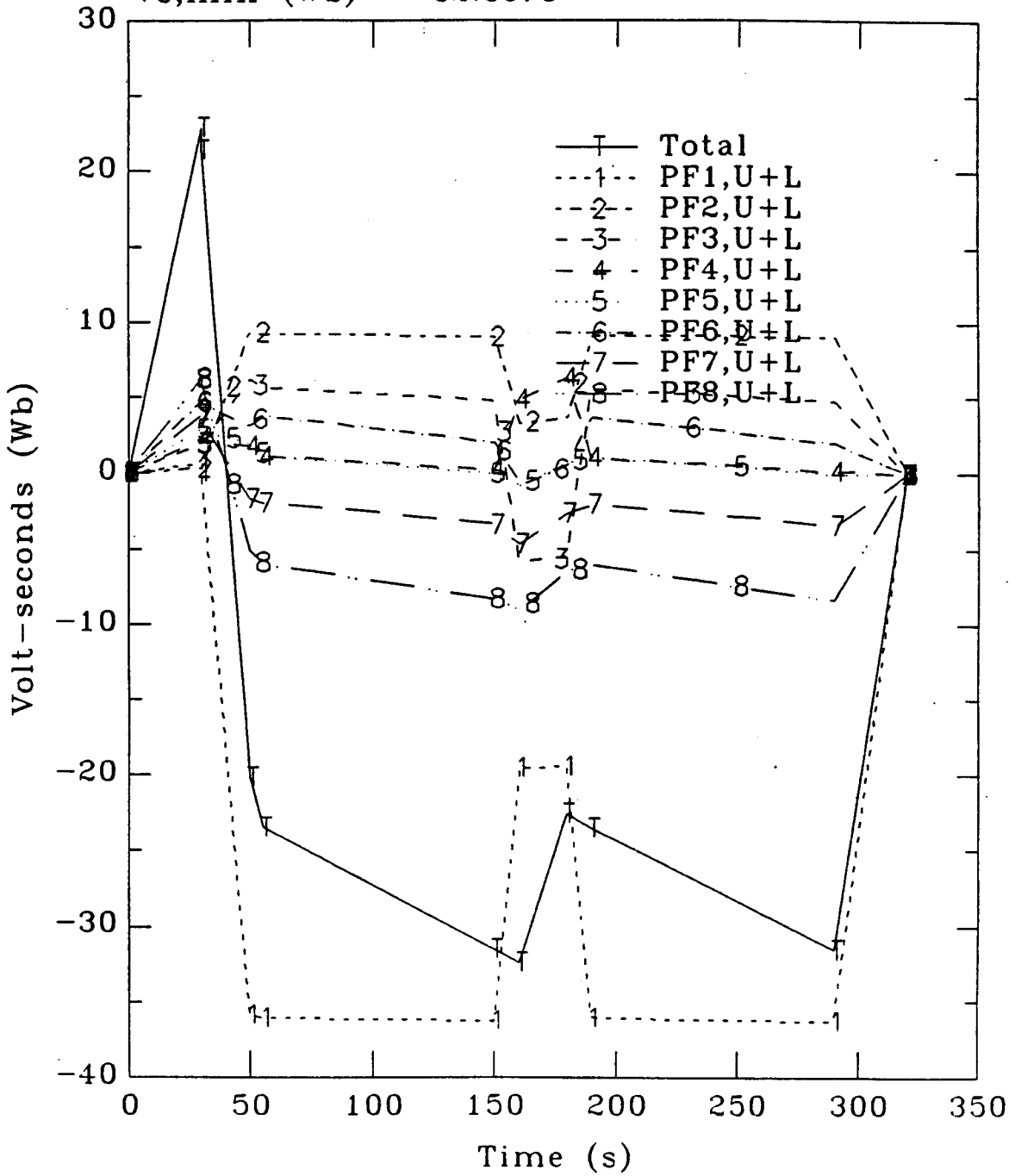
Figure 6

PF Coil contributions to Plasma Flux in RF Reset Scenario
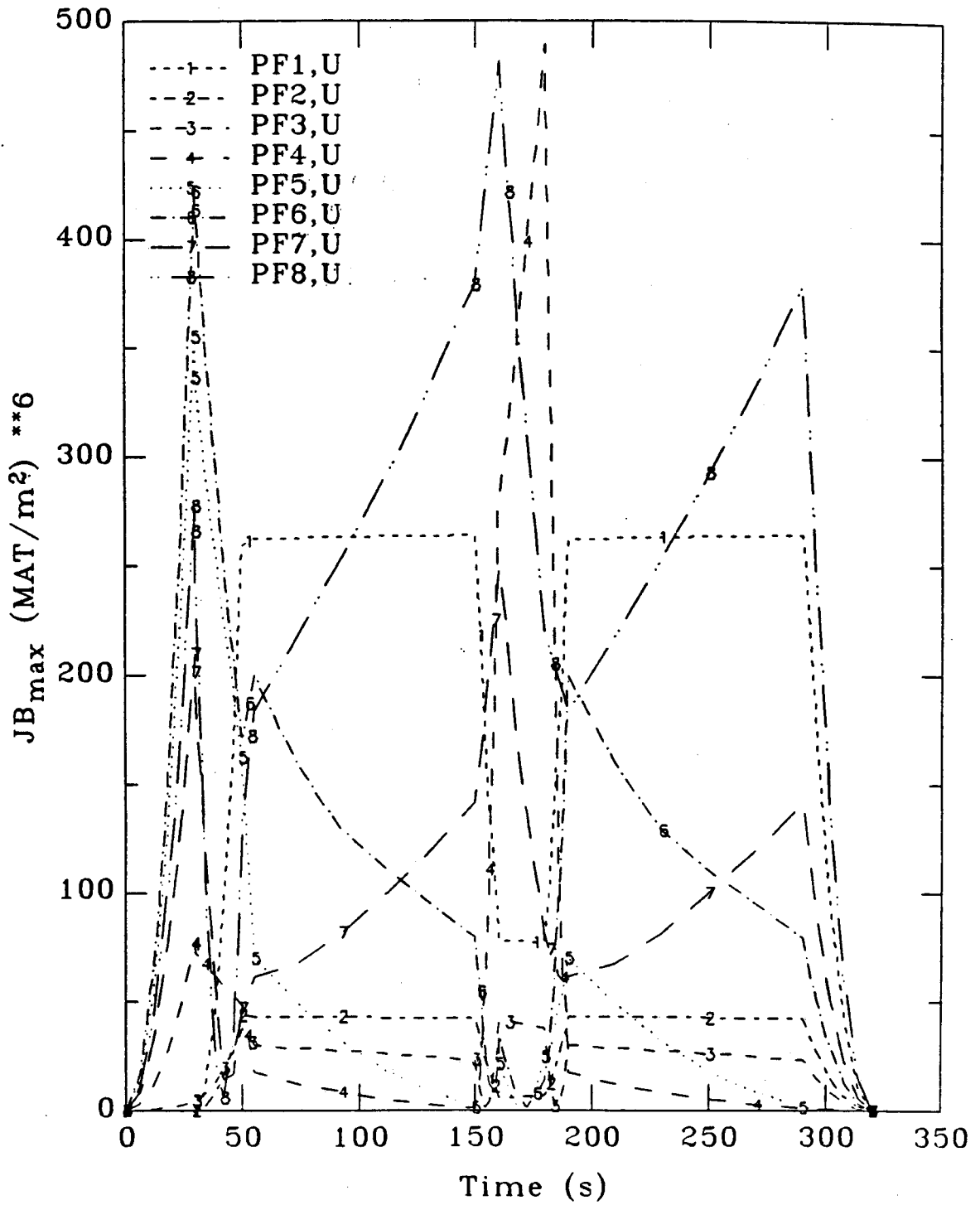
Figure 7

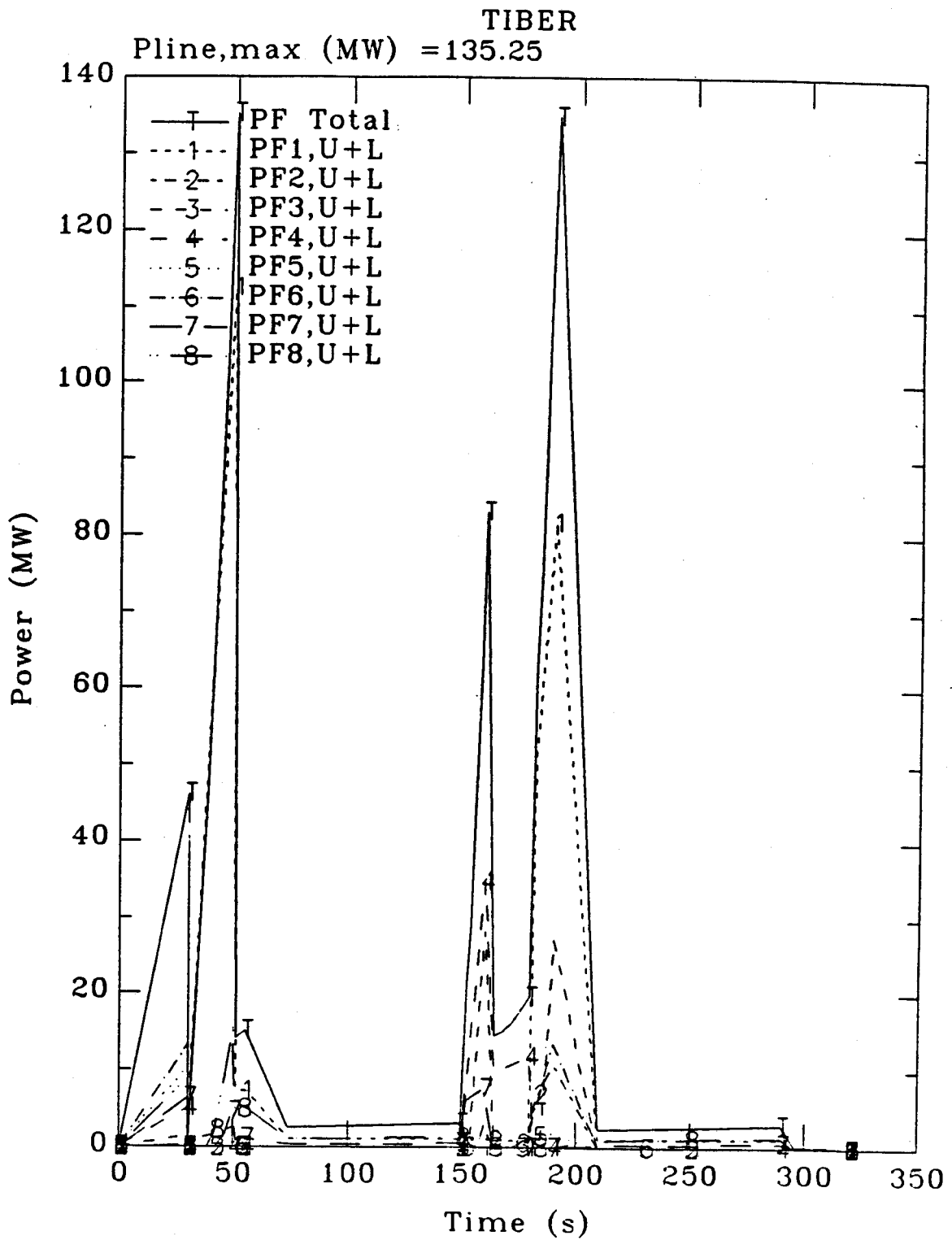JB_{max} **Product in PF Coils (MA-T/m^2) vs. Time (s)**

Figure 8
PF Power Supply Requirements, Scenario with RF Reset

The average tensile, axial and Tresca membrane stresses in the ICCS conduits were calculated as functions of time for each of the PF coils. As expected, none of the coils have to endure a complete stress cycle during the reset period. However, for some of the coils, the reduction in stress cycling is disappointing. When PF1 adjusts to the collapse of plasma thermal pressure during recycling, its stresses drop substantially, as shown in Fig. 9. The peak Tresca stress of 725 MPa is reduced to 300 MPa during the recycling period. The average Tresca membrane stress in the conduits in the central solenoid varies from 600 MPa to 300 MPa during plasma reset, but reaches a one-time peak of 700 MPa at the beginning of initiation. The reduction of fatigue cycling then is more substantial for the critical central solenoid than for the PF1 coil.

5.0 Conclusions

• Scenarios have been developed for a variety of TIBER/ITER options, satisfying a broad range of physics and engineering constraints.

• The TIBER design is not capable of long-pulse, full-current burn without some rf assist. However, it is capable of a 10 V-s burn at 8 MA in full ohmic operation and a 20 V-s ohmic burn with some rf assist during start-up.

• The PF system provides an 8 V-s ohmic burn at 8 MA for a low-beta, current-driven reset. This improves but does not eliminate the problem of high-cycle fatigue in the PF coils.
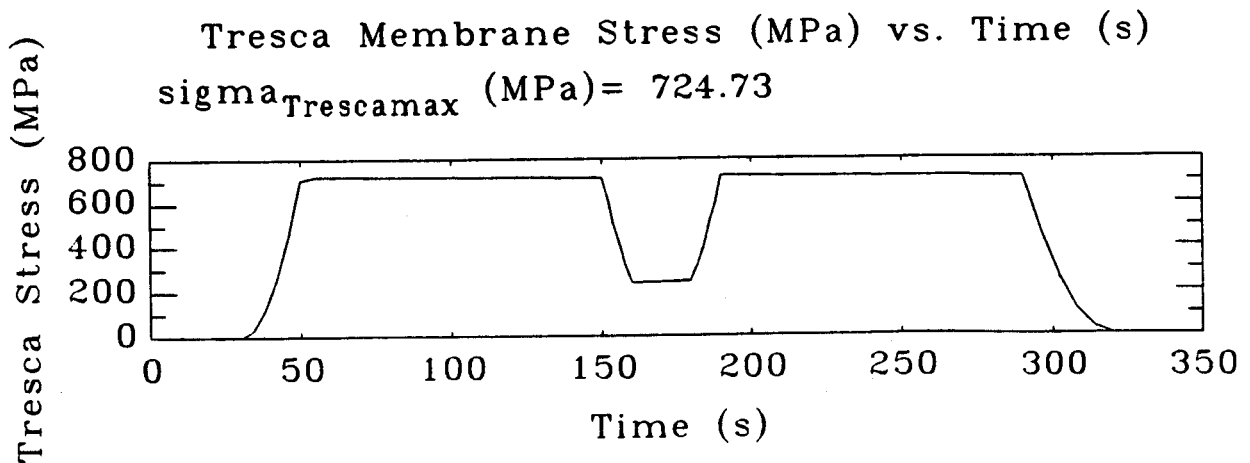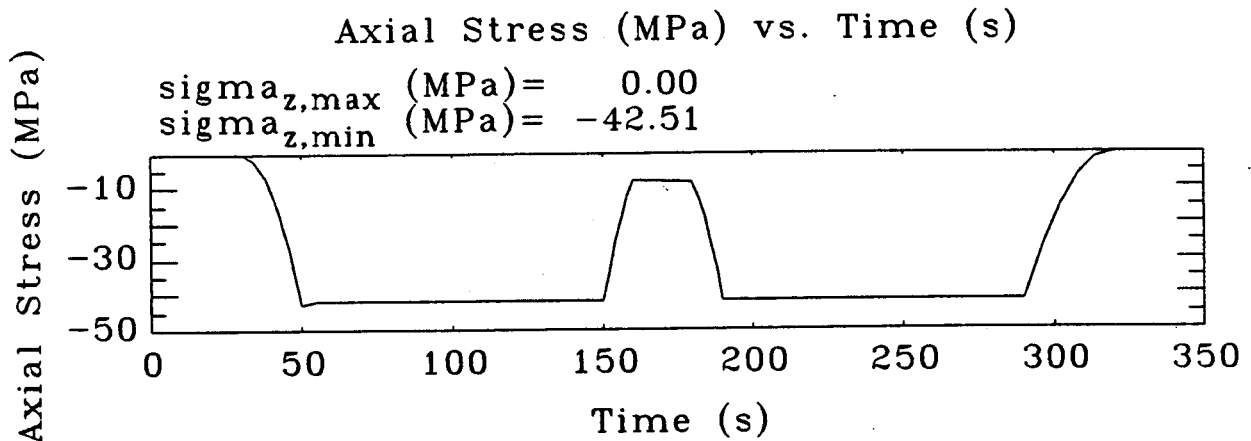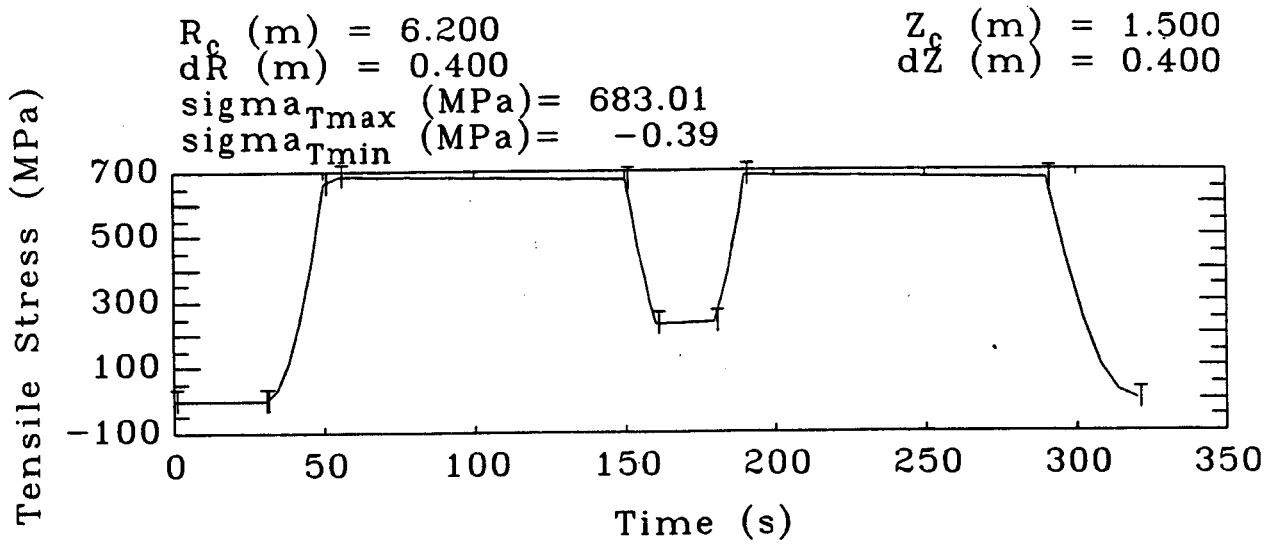
Fig. 9 – Membrane Stress in PF1 Conduit (MPa) vs. Time (s)

References

[HE85] C.D. Henning and B.G. Logan et al., 'TIBER Final Design Report,' LLL UCID-20589, Nov 1985.

[PP84] Princeton Plasma Physics Laboratory, 'TFCX: Preconceptual Design Specification, *Addendum to the Preconceptual Design Report*,' TFCX F-Axxx-8406-004, June 15, 1984.

[PI85] R.D. Pillsbury, Jr., R.J. Thome, J.M. Tarrh and W.R. Mann, 'Poloidal Field Coil System Design Using a Field Expansion Technique,' Proc MT-9 Conference on Magnet Technology, SIN, Zurich, SW, Sept 1985.

[SU85] M. Suenaga, DOE Workshop on Conductor-Sheath Issues for ICCS, Germantown, MD, July 15-16, 1985.